

# Radiative Equilibrium of the Earth's Atmosphere 1. The Grey Case

著者	Yamamoto Giichi
雑誌名	Science reports of the Tohoku University. Ser. 5, Geophysics
巻	5
号	2
ページ	45-57
発行年	1953-10
URL	<a href="http://hdl.handle.net/10097/44502">http://hdl.handle.net/10097/44502</a>

# *Radiative Equilibrium of the Earth's Atmosphere 1.*

## *The Grey Case*

By Giichi YAMAMOTO

Geophysical Institute, Faculty of Science, Tôhoku University

(Received 27 August 1953)

### *Abstract*

In the present paper the fourth approximate solution of the equation of radiative equilibrium of the grey case with finite optical thickness was obtained with use of the method of discrete ordinate extended by CHANDRASEKHAR. One of the characteristics of the solution is that the smaller the total optical thickness of the absorbing medium the higher its equilibrium temperature at the top of the medium. With application of the solution to the earth's atmosphere whose absorbing medium was assumed to be water vapor with grey absorption coefficient, some characteristics of the stratosphere, i.e., the decrease of the tropopause height and the increase of the tropopause temperature with increasing latitude, are explained by the decrease of water vapor content in the atmosphere with increasing latitude.

### **I. Introduction**

By the recent works on radiative transfer in the earth's atmosphere, it is becoming clear that the stratospheric temperature distribution is maintained by the heat balance due to the infrared radiative transfer of three absorbing media, i.e., water vapor, carbon dioxide and ozone, and to the absorption of solar radiation by ozone. It is further clarified by STRONG and PLASS [7] that the pressure broadening of infrared absorption lines has important stabilizing effect not only on the stratosphere but also on the troposphere, by permitting the radiation emitted from the wings of lines in the lower atmosphere where the lines have greater half-width to pass through the upper layers where the lines have smaller half-width. Under these circumstances it may seem out of fashion to return to the classical problem of radiative equilibrium in the grey case. In recent years, however, the problem in the grey case was thoroughly investigated by a number of astrophysicists whose efforts have led to many approximate solutions and even exact one in the case of semi-infinite atmosphere. Nevertheless, in the case of the terrestrial atmosphere of finite thickness the solution has not so much been improved on the pioneer work of EMDEN [3] which is only of the first approximation with errors of, probably, more than 15 per cent. And it is regrettable that one of the essential characteristics of the solution in the case of the finite atmosphere that the smaller the total content of the absorbing medium in the atmosphere the higher the equilibrium temperature at the top of the atmosphere, which seems to be useful for the interpretation of the temperature distribution of the terrestrial atmosphere, and of which EMDEN had paid a short glance, had remained unnoticed by other workers.

In the present paper the author has obtained the fourth approximate solution of

the problem based on the method of discrete ordinates extended by CHANDRASEKHAR [1] and has shown that the decrease of the tropopause height and the increase of the tropopause temperature with increasing latitude are explained with use of the solution to the case of the earth's atmosphere with assumption that its absorbing medium is water vapor with grey absorption coefficient.

## 2. The Problem and its Approximate Solution.

In the grey case on radiative equilibrium the transfer equation for the integrated radiation is given by

$$\mu \frac{dI(\tau, \mu)}{d\tau} = I(\tau, \mu) - \frac{1}{2} \int_{-1}^{+1} I(\tau, \mu) d\mu, \quad (1)$$

where  $I(\tau, \mu) = \int_0^\infty I_\nu d\nu$  ( $\nu$  = frequency) is the integrated intensity,  $\tau = \int_z^\infty k\rho dz$  is the optical thickness measured from the top of the atmosphere inward,  $k$  is the absorption coefficient,  $\rho$  is the density of the absorbing medium,  $\mu = \cos \theta$  and  $\theta$  is the angle which the pencil of  $I(\tau, \mu)$  at the depth  $\tau$  makes with the outward drawn normal. Suppose that we consider separately the propagation of each of the  $2n$  'rays' which travel in the directions determined by  $-\mu_n, -\mu_{n-1}, \dots, -\mu_1, \mu_1, \dots, \mu_{n-1}, \mu_n$ , then we can replace the equation of transfer (1) by the system of  $2n$  linear equations

$$\mu_i \frac{dI_i(\tau)}{d\tau} = I_i(\tau) - \frac{1}{2} \sum_j a_j I_j(\tau) \quad (i = \pm 1, \pm 2, \dots, \pm n), \quad (2)$$

where the  $a_j$ 's ( $i = 1, 2, \dots, n$ ) are the known weights appropriate for a quadrature formula based on the division ( $\mu_i$ ) of the interval  $(-1, +1)$ . The general solution of the system of equations (2) can be written in the form

$$I_i(\tau) = b \left\{ \sum_{\alpha=1}^{n-1} \frac{L_{-\alpha} e^{-k_\alpha \tau}}{1 + \mu_i k_\alpha} + \sum_{\alpha=1}^{n-1} \frac{L_{-\alpha} e^{+k_\alpha \tau}}{1 - \mu_i k_\alpha} + \tau + \mu_i + Q \right\}, \quad (3)$$

where  $\pm k_\alpha$  are the  $2(n-1)$  roots of the characteristic equation

$$\frac{1}{2} \sum_i \frac{a_i}{1 + \mu_i k} = 1, \quad (4)$$

and  $b, L_{\pm\alpha}$  ( $\alpha = 1, 2, \dots, n-1$ ) and  $Q$  are the  $2n$  constants of integration which can be determined from the boundary conditions.

The boundary conditions appropriate for the planetary atmosphere will be as follows. At the top of the atmosphere, there will be no inward radiation. Hence we have

$$I_i(0) = 0 \quad \text{for } \mu_i < 0. \quad (5)$$

At the surface of the planet, the outward radiation may be assumed to be the isotropic black radiation corresponding to the surface temperature. Let the optical thickness down to the surface be  $\tau_1$ , the radiation irradiated by the surface be  $I_s$  and the surface temperature be  $T_s$ , then we have

$$I_i(\tau_1) = I_s = \frac{\sigma T_s^4}{\pi} \quad \text{for } \mu_i > 0, \quad (6)$$

where  $\sigma$  is STEFAN'S constant. The constants  $b, L_\alpha, L_{-\alpha}$  and  $Q$  are determined by (3) and the linear systems (5) and (6), i.e., by

$$Q - \mu_i + \sum_a \frac{L_a}{1 - \mu_i k_a} + \sum_a \frac{L_{-a}}{1 + \mu_i k_a} = 0. \quad (7)$$

$$\tau_1 + Q + \mu_i + \sum_a \frac{L_a e^{-k_a \tau_1}}{1 + \mu_i k_a} + \sum_a \frac{L_{-a} e^{+k_a \tau_1}}{1 - \mu_i k_a} = \frac{I_s}{b}. \quad (8)$$

$$\left. \begin{array}{l} \{ \alpha = 1, 2, \dots, n-1 \} \\ \{ i = 1, 2, \dots, n \} \end{array} \right\}.$$

By the addition of (7) and (8) we have

$$\sum_a (L_a + L_{-a} e^{+k_a \tau_1}) \left\{ \frac{1}{1 - \mu_i k_a} + \frac{e^{-k_a \tau_1}}{1 + \mu_i k_a} \right\} = \frac{I_s}{b} - \tau_1 - 2Q \quad (9)$$

$$\left. \begin{array}{l} \{ \alpha = 1, 2, \dots, n-1 \} \\ \{ i = 1, 2, \dots, n \} \end{array} \right\}.$$

Hence, we have

$$L_{-a} = -L_a e^{-k_a \tau_1} \quad (10)$$

$$b = \frac{I_s}{\tau_1 + 2Q} \quad (11)$$

provided  $\frac{1}{1 - \mu_i k_a} + \frac{e^{-k_a \tau_1}}{1 + \mu_i k_a} \neq 0$ . With substitute of (10) in (7), we have the linear system of equations to determine the remaining constants  $L_a$  and  $Q$ ,

$$Q - \mu_i + \sum_a L_a \left( \frac{1}{1 - \mu_i k_a} - \frac{e^{-k_a \tau_1}}{1 + \mu_i k_a} \right) = 0, \quad (12)$$

$$\left. \begin{array}{l} \{ \alpha = 1, 2, \dots, n-1 \} \\ \{ i = 1, 2, \dots, n \} \end{array} \right\},$$

and the solutions (3) are now expressed as

$$I(\tau, \mu_i) = \frac{I_s}{\tau_1 + 2Q} \left[ \tau + Q + \mu_i + \sum_a \frac{L_a e^{-k_a \tau}}{1 + \mu_i k_a} + \sum_a \frac{L_a e^{-k_a(\tau_1 - \tau)}}{1 - \mu_i k_a} \right]. \quad (13)$$

The source function  $B(\tau) = \int_0^{\infty} B_\nu(\tau) d\nu$  ( $B_\nu$  = PLANCK'S function) is given by

$$B(\tau) = \frac{1}{2} \int_{-1}^{+1} I(\tau, \mu) d\mu = \frac{1}{2} \sum_i a_i I(\tau, \mu_i). \quad (14)$$

With substitute of (13) in (14) and with reference to (4) and to the known relations:

$$\sum_i a_i = 2, \quad \sum_i a_i \mu_i = 0, \quad \sum_i a_i \mu_i^2 = \frac{2}{3} \quad (\text{c. f. [5]}) \quad (15)$$

we have

$$B(\tau) = \frac{I_s}{\tau_1 + 2Q} \left[ \tau + Q + \sum_a L_a (e^{-k_a \tau} - e^{-k_a(\tau_1 - \tau)}) \right]. \quad (16)$$

If we denote the temperature of the layer of the optical thickness  $\tau$  to be  $T$ , then by means of STEFAN'S law  $B(\tau) = B(T(\tau)) = \frac{\sigma T^4}{\pi}$ , so that by (6) and (16) the temperature distribution in the atmosphere of radiative equilibrium is given by

$$T^4 = \frac{T_s^4}{(\tau_1 + 2Q)} \left[ \tau + Q + \sum_a L_a (e^{-k_a \tau} - e^{-k_a(\tau_1 - \tau)}) \right]. \quad (17)$$

Now the flux of radiation which is supposed to have a given value  $F$  is expressed by

$$F = 2 \int_{-1}^{+1} I(\tau, \mu) \mu d\mu = \sum_i a_i I(\tau) \mu_i. \quad (18)$$

It is easily found, on using (13), (15) and the relation

$$\sum_i \frac{a_i \mu_i}{1 + \mu_i k} = 0, \quad (k = \pm k_a) \quad (19)$$

which results immediately from (4), that the approximate expression  $2 \sum_i a_i I_i(\tau) \mu_i$  is independent of  $\tau$  and that

$$F = \frac{4}{3} \frac{I_s}{\tau_1 + 2Q}. \quad (20)$$

Now from (16) the following interesting relations are derived, i.e.,

$$B(\tau) + B(\tau_1 - \tau) = B(0) + B(\tau_1) = 2B(\tau_1/2) = I_s. \quad (21)$$

Equations (16), (17), (20) and (21) reveal following characteristics of the temperature distribution of the finite atmosphere in radiative equilibrium.

1. There is a discontinuity of temperature between the boundary surface and the air just above it. If we denote the temperature of the lowest layer just above the boundary surface be  $T_1$ , then by the relation,  $B(\tau_1) = \sigma T_1^4 / \pi$  and by (6) and (21) we have  $T_1 < T_s$ . This fact was originally noticed by EMDEN. The physical meaning will be as follows. It is well known that the black surface is essentially equivalent to the semi-infinite layers with the same temperature, and it is also known that in the semi-infinite atmosphere in radiative equilibrium  $B(\tau)$  increases with increase of  $\tau$  unlimitedly. In this semi-infinite case the radiation, which originates from the lower layers and pass through the surface at  $\tau = \tau_1$  outwardly, is necessarily larger than the black radiation corresponding to the temperature at  $\tau = \tau_1$ . Now the former radiation is the very radiation emitted by the boundary surface in order that the condition of radiative equilibrium be maintained between the boundary surface and the atmosphere above it. Hence there must be a temperature discontinuity between the boundary and the air above it unless the optical thickness of the air column is extremely large.

2. The curve of the normalized source function,  $B(\tau)/I_s$ , as function of  $\tau$  has the twofold axis of symmetry through the point at  $\tau = \tau_1/2$ , that is, a half of the curve in the range of  $\tau = \tau_1/2$  to  $\tau = \tau_1$  coincides with the other half by the rotation of the curve by  $180^\circ$  about the axis through the point at  $\tau = \tau_1/2$ . This property which is shown by (21) is useful in numerical calculation of the source function.

3. We can know by (16) that the value of  $B(\tau)/I_s$  covers nearly the total range from 0 to 1 when the total optical thickness  $\tau_1$  is extremely large, and the range, which the value of  $B(\tau)/I_s$  can take, decreases with decrease of the value of  $\tau_1$ , and in the extreme case of the zero optical thickness the value of  $B/I_s$  concentrates to  $1/2$ . Corresponding relation also holds to the value of  $T/T_s$  by (17). It will be shown later that this property is of importance in the explanation of the change of the temperature distribution with latitude in our atmosphere where the decrease of the water vapor content with increasing latitude is considerable. In the extreme case of the non-absorbing atmosphere the temperature is  $T_s/\sqrt{2}$  or  $0.841 T_s$  throughout the air column.

4. Equation (20) shows us that the normalized flux  $F/I_s$  decreases with increase of  $\tau_1$ .

### 3. Numerical Calculation.

In carrying out the approximate calculation by the method of discrete ordinate, the choice of the quadrature formula is of some importance in the sense that how well the lowers of approximation ( $\mu = 3$  or  $4$ ) represent the solution. In the case of the semi-

infinite atmosphere KOURGANOFF [5] has shown that the NEWTON-COTES quadrature formula is preferable to that of GAUSS in this contexts. For instance, in the fourth approximation, the fractional errors of  $B(\tau)$ , i.e.,  $|AB(\tau)|/B_s(T)$ , where  $B_s(T)$  is the true value of  $B(T)$ , are smaller than about one percent when the NEWTON-COTES formula is used, while they are smaller than about two percent when the GAUSS formula is used. On this account we have chosen the NEWTON-COTES quadrature formula in our calculation.

In the fourth approximation, the points of subdivision in the NEWTON-COTES method are  $\mu_1 = 1/7$ ,  $\mu_2 = 3/7$ ,  $\mu_3 = 5/7$ ,  $\mu_4 = 1$ , and the corresponding weights are

$$a_1 = 0.34595, \quad a_2 = 0.15313, \quad a_3 = 0.41400, \quad a_4 = 0.08692.$$

The three positive roots of the characteristic equation (4) are found to be

$$k_1 = 1.07510, \quad k_2 = 2.13782, \quad k_3 = 5.74411.$$

The values of constants  $Q$ ,  $L_1$ ,  $L_2$ ,  $L_3$ , for several values of  $\tau_1$  are shown in Table. 1.

Table 1. The values of  $Q$ ,  $L_1$ ,  $L_2$ , and  $L_3$  for several values of  $\tau_1$

$\tau_1$	$Q$	$L_1$	$L_2$	$L_3$
0.1	0.683006	-0.018721	-0.027213	-0.096926
0.25	0.694286	-0.018558	-0.026829	-0.094656
0.5	0.701650	-0.018436	0.026488	-0.092949
1	0.708600	-0.018364	-0.026400	0.092222
2.5	0.712798	-0.018319	-0.026308	-0.091788
5	0.713519	-0.018312	-0.026294	-0.091725

With increase of the value of  $\tau_1$  the value of  $Q$  increases and the absolute values of  $L_1$ ,  $L_2$  and  $L_3$  decrease. The corresponding values of  $B(\tau)/I_s$ ,  $F/I_s$ , and  $T/T_s$  are given in Table 2. The graphs of  $B(\tau)/I_s$  and  $T/T_s$  as function of  $\tau$  are also shown in Fig. 1 and Fig. 2. From the table and the figures we can well understand the characteristic features of the finite atmosphere described qualitatively in the previous section.

Table 2 The values of  $B(\tau)/I_s$ ,  $F/I_s$  and  $T/T_s$ .

$\tau_1 = 0.1 \quad F/I_s = 0.909497$			$\tau_1 = 0.25 \quad F/I_s = 0.813717$		
$\tau/\tau_1$	$B(\tau)/I_s$	$T/T_s$	$\tau/\tau_1$	$B(\tau)/I_s$	$T/T_s$
0.0	0.43213	0.81078	0.0	0.37024	0.78005
0.1	0.44582	0.81712	0.1	0.39726	0.79391
0.2	0.45943	0.82329	0.2	0.42356	0.80673
0.3	0.47299	0.82930	0.3	0.44933	0.81873
0.4	0.48650	0.83517	0.4	0.47475	0.83007
0.5	0.50000	0.84090	0.5	0.50000	0.84090
0.6	0.51350	0.84652	0.6	0.52525	0.85132
0.7	0.52701	0.85203	0.7	0.54957	0.86200
0.8	0.54057	0.85746	0.8	0.57644	0.87134
0.9	0.55418	0.86281	0.9	0.60274	0.88111
1.0	0.56787	0.86809	1.0	0.62976	0.89083

$\tau_1 = 0.5 \quad F/I_s = 0.700538$ 

$\tau/\tau_1$	$B(\tau)/I_s$	$T/T_s$
0.0	0.30941	0.74582
0.1	0.35156	0.77002
0.2	0.39088	0.79024
0.3	0.42826	0.80896
0.4	0.46442	0.82552
0.5	0.50000	0.84090
0.6	0.53558	0.85547
0.7	0.57174	0.86956
0.8	0.60912	0.88344
0.9	0.64865	0.89692
1.0	0.69059	0.91160

 $\tau_1 = 1 \quad F/I_s = 0.551602$ 

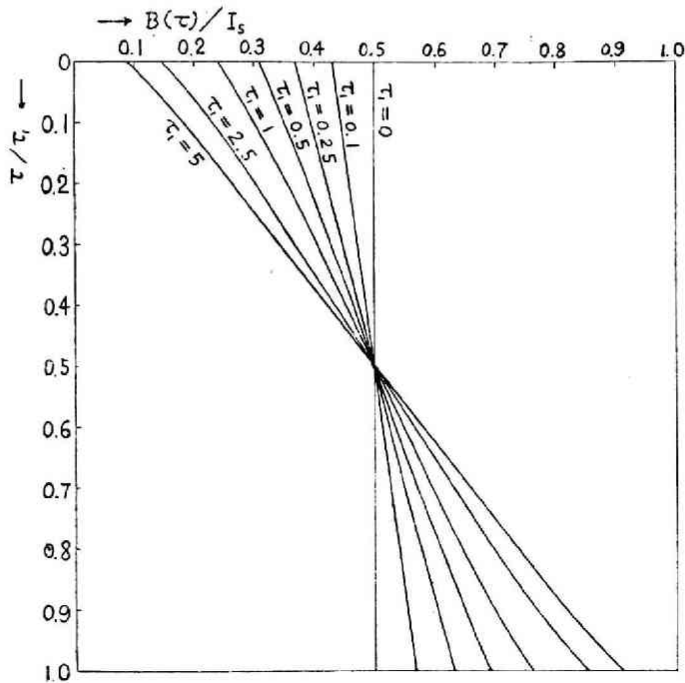
$\tau/\tau_1$	$B(\tau)/I_s$	$T/T_s$
0.0	0.24048	0.69987
0.1	0.30209	0.74137
0.2	0.35613	0.77251
0.3	0.40591	0.79819
0.4	0.45344	0.82060
0.5	0.50000	0.84090
0.6	0.54656	0.85982
0.7	0.59409	0.87794
0.8	0.64388	0.89578
0.9	0.69791	0.91401
1.0	0.75952	0.93355

 $\tau_1 = 2.5 \quad F/I_s = 0.339651$ 

$\tau/\tau_1$	$B(\tau)/I_s$	$T/T_2$
0.0	0.14718	0.61939
0.1	0.23268	0.69453
0.2	0.30323	0.74207
0.3	0.36976	0.77979
0.4	0.43507	0.81216
0.5	0.50000	0.84090
0.6	0.56493	0.86696
0.7	0.63025	0.89100
0.8	0.69677	0.91363
0.9	0.76732	0.93593
1.0	0.85282	0.96098

 $\tau_1 = 5 \quad F/I_s = 0.207457$ 

$\tau/\tau_1$	$B(\tau)/I_s$	$T/T_s$
0.0	0.08982	0.54745
0.1	0.18496	0.65580
0.2	0.26515	0.72256
0.3	0.34374	0.76570
0.4	0.42194	0.80596
0.5	0.50000	0.84090
0.6	0.57807	0.87196
0.7	0.65626	0.90005
0.8	0.73485	0.92587
0.9	0.81504	0.95016
1.0	0.91018	0.97675

Fig. 1. The graphs of  $B(\tau)/I_s$  as function of  $\tau/\tau_1$ .

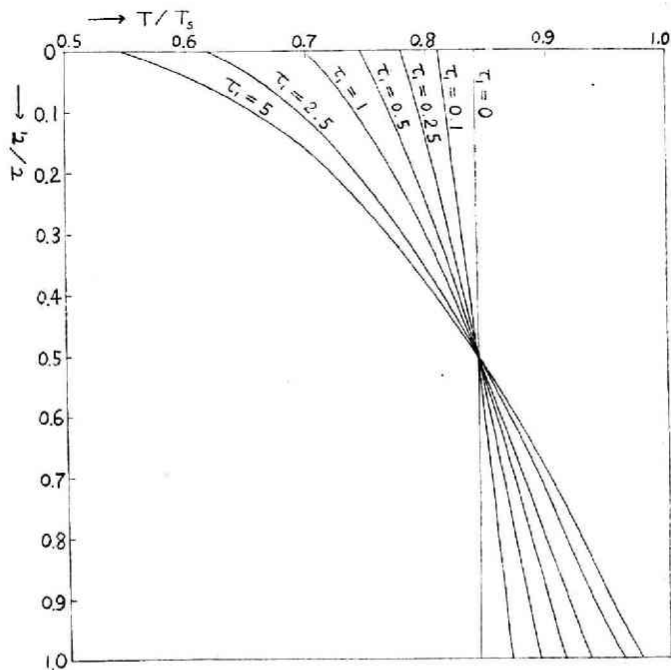


Fig. 2. The graphs of  $T/T_s$  as function of  $\tau/\tau_s$ .

**4. Application of the Results to the Earth's Atmosphere.**

We will now consider the application of the above results to the earth's atmosphere under the assumption that it is in radiative equilibrium. In this case some difficulty arises in regard to the determination of the mean absorption coefficient of the absorbing medium. Although astrophysicists suggest several ways of defining the mean absorption coefficient of the non-grey absorber, meteorologists know that the matter is very complicated in our atmosphere in the point that we are concerned with three absorbing media; i.e., water vapor, carbon dioxide and ozone, the absorption bands of which are composed of many lines whose widths vary with pressure. In the classical investigation of EMDEN, the mean absorption coefficient  $k$  for the infrared region was assumed to be  $2k = 2.3$ . However, there seems to be no theoretical or experimental reason to support the value. For instance, according to YAMAMOTO [8], the mean transmission curve of water vapor at 300°K for the whole infrared region is as shown in Fig.3 (c.f. Table 2 of

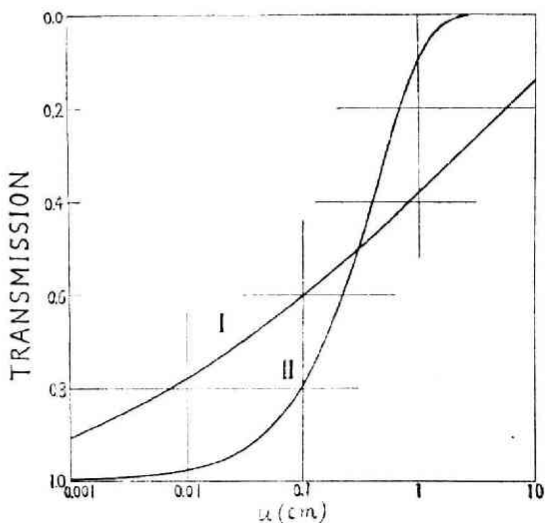


Fig. 3. Curve I : Mean transmission curve of water vapor at 300° K for the whole infrared region.  
Curve II :  $e^{-2ku}$  with  $2k = 2.3$ .



YAMAMOTO's paper), and the corresponding transmission curve in EMDEN's treatment of the problem, which is known to be  $e^{-2ku}$ , ( $u$  is the water vapor content) is also shown in Fig. 3 with  $2k = 2.3$ . It will be seen from the figure that both transmission curves meet only at one point with  $u = 0.3$ . We can draw many similar exponential curves as EMDEN's with other values of  $k$ , and there is no reason that the curve with  $2k = 2.3$  is preferable to other curves. In my opinion the most preferable value of the absorption coefficient of BEER's sense in the grey case, which is assumed instead of the actual absorption law, will be determined to be such as to give a reasonable stratosphere temperature when it is used in the actual calculation. The choice of the value of  $k$  will be done, necessarily, by trial and error method for the assumed atmosphere. In the present investigation water vapor alone was assumed as the absorbing medium and the existences of carbon dioxide and ozone were neglected. To calculate the equilibrium temperature distribution we must further assume the vertical and the latitudinal distributions of water vapor and the latitudinal distribution of the surface temperature. The latter quantity is needed to give the boundary condition expressed by (6). Physically it means that the earth surface temperature is governed not only by the infrared radiation but also by the absorption of the solar radiation which is given as the outer condition in the strict sense. In the present investigation these necessary quantities were selected to match the model atmosphere which was proposed by LONDON [6] for March, northern hemisphere. The water vapor

Table 3. The assumed model atmosphere and the calculated temperature distribution.

$$u = \int_0^p \frac{q}{g} dp, \quad \tau = ku. \quad \text{The assumed value of } k \text{ is } 0.5.$$

0-10°N. $T_s = 300.9$			20-30°N. $T_s = 299.5$		
Level (km)	$u$	$T$	Level (km)	$u$	$T$
0	4.9072	288.0	0	2.8236	279.2
1	3.1072	263.5	1	1.6686	254.1
2	1.9638	244.8	2	0.8926	235.2
3	1.2390	229.8	3	0.5162	223.5
4	0.7590	217.7	4	0.2821	213.6
5	0.4408	207.5	5	0.1559	207.4
7	0.13306	194.6	7	0.04306	201.5
9	0.03406	189.3	9	0.01056	199.4
11	0.00682	187.6	11	0.00292	198.8
13	0.00123	187.3	13	0.00092	198.7
15	0.00015	187.2	15	0.00022	198.7
$\infty$	0	187.2	$\infty$	0	198.7

40-50°N. $T_s = 277.2$			60-70°N. $T_s = 258.9$		
Level (km)	$u$	$T$	Level (km)	$u$	$T$
0	1.1780	253.7	0	0.3178	227.2
1	0.7698	239.4	1	0.2166	221.4
2	0.4604	227.9	2	0.1328	216.1
3	0.2489	218.5	3	0.08732	213.1
4	0.1302	212.2	4	0.04758	210.1
5	0.06635	208.5	5	0.02973	208.7
7	0.01628	205.3	7	0.01138	207.1
9	0.00436	204.4	9	0.00286	206.4
11	0.00149	204.2	$\infty$	0	206.1
$\infty$	0	204.1			

data used were, however, not LONDON'S original data which include the pressure correction as proportional to square root of the pressure. The data actually used were those without pressure correction, which were calculated from LONDON'S data by the formula;  $u = \int_z^{\infty} \rho_w dz = \int_0^p q/gdp$ , where  $\rho_w$  is the density of water vapor,  $q$  the specific humidity,  $g$  the acceleration of gravity, and  $p$  the pressure, and which were listed in Table 3. The assumed values of the surface temperature shown in Table 3 were also taken from LONDON'S table. Now assuming several values of  $k$ , the computation of the temperature distribution was carried out, of which the most reasonable one was shown in Table 3, which corresponds to  $k = 0.5$ . With a larger value of  $k$  than this, the calculated stratosphere temperature becomes too low to be valid, and with a smaller value of  $k$  than this, the calculated stratosphere temperature becomes too high to be valid. The temperature distributions listed in Table 3 are shown graphically in Fig. 4. It will be seen from the table that there is a marked temperature discontinuity at the surface at each latitude, which was already noticed by EMDEN, and from the figure that the trend of each temperature curve is similar to EMDEN'S curve, that is to say, the lapse rate is considerably large at lower levels and it diminishes with increase of height and at upper levels there exists nearly isothermal state. The following characteristics of the temperature variation with respect to latitude were not noticed so far:

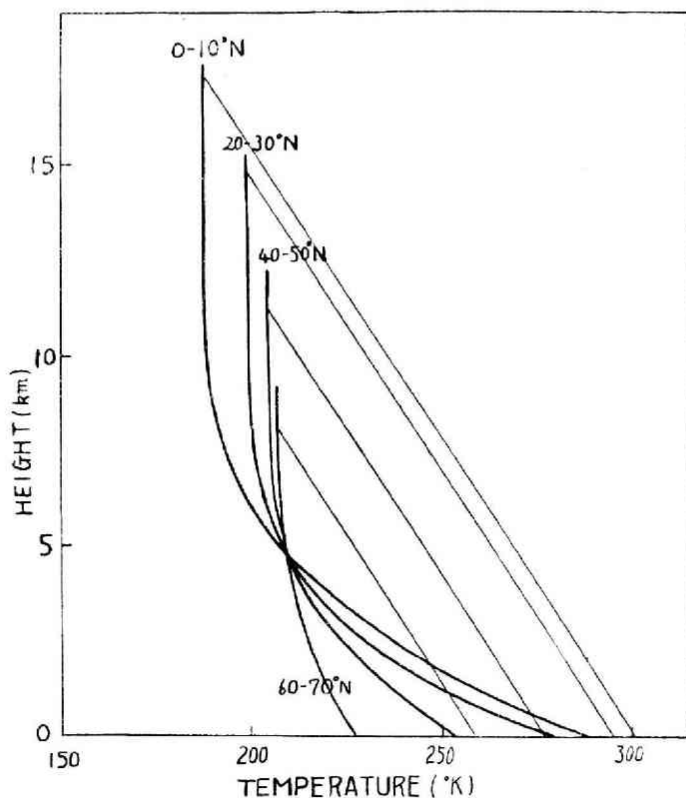


Fig. 4. The calculated temperature distribution. The straight lines are those with lapse-rate of 6.5°C/km starting from the earth surface temperature.

1. The temperature discontinuity at the surface increases with increase of latitude, i.e., with decrease of the total optical thickness  $\tau_1$ .
2. The lapse rate of temperature at any given height decreases with increase of latitude.
3. The temperature of a given upper level (above about 5 km) increases with increase of latitude.

In a word it will be said that the temperature profile in the atmosphere, except at the surface discontinuity, tends to be uniform with increasing latitude, or with decrease of the total optical thickness of the air, as was described qualitatively in section 2. Fig. 4 shows that at  $60 \sim 70^\circ N$  the lapse rate is far smaller than the dry adiabatic lapse rate even at lowest levels of the atmosphere. However, the temperature discontinuity at the surface in this case is as large as  $33^\circ C$ , so that the air column becomes eventually unstable in the lower parts of the column. It was shown by YAMAMOTO [9] that in the actual troposphere the temperature is so distributed as to be in radiato-convective equilibrium; that is, the net heat flux is maintained to be constant in part by the action of turbulence and in part by the action of radiation, and the result is that the lapse rate is about  $6.5^\circ C/km$  in steady state. Upon this consideration, if we define the tropopause as the intersecting point of the calculated temperature profile and the line of the constant lapse rate of  $6.5^\circ C/km$  starting from the earth surface temperature, then we have from Fig. 2 the height and the temperature of the tropopause at each air column as shown in Table 4.

Table 4. The height and the temperature of the tropopause for March, northern hemisphere.

Latitude	Height (km)		Temperature ( $^\circ K$ )	
	Observed	Calculated	Observed	Calculated
0 - $10^\circ N$	16.0	17.4	197.5	187.2
20 - $30^\circ N$	16.0	14.9	201.4	198.7
40 - $50^\circ N$	11.0	11.3	218.0	204.2
60 - $70^\circ N$	10.0	8.1	220.7	206.8

Note. Observed values are due to LONDON.

The height of the tropopause, thus defined, decreases with increase of latitude and its temperature increases with increase of latitude. Although the numerical values shown in Table 4 do not necessarily coincide with those of the actual atmosphere, the characteristic feature with respect to the latitudinal variation of the height and the temperature of the tropopause is quite similar to what actually happens in nature. Hitherto, this variation of the tropopause was explained in the one hand by DOBSON, BREWER and CWILONG [2] as the effect of the variation of ozone content with latitude, and on the other hand by GOODY [4] by considering the cooling effect of water vapor and the heating effect of carbon dioxide and the variations of these effects with latitude. Upon my calculation it is shown that the chief cause of the variation of the tropopause height and its temperature lies in the fact that the total water vapor content in the air column decreases with increase of latitude. As to the more detailed explanation of the discrepancy between the observed and the calculated tropopause temperature to be seen in Table 4; the latter being generally lower than the former, it will be needed

to take into account of the heating effect of ozone. In this connexion the qualitative argument of DOBSON, BREWER and CWILONG [2] is in good sense to remedy the discrepancy.

Under the assumption of the grey atmosphere we cannot go further. To the more complete explanation of not only the tropopause features described above but also other stratospheric features, for instance, the increase of the temperature with height and the phase difference between the stratospheric and the tropospheric temperature noticed by DOBSON, BREWER and CWILONG [2], we are forced to attack the more complicated problem of taking into account of the effect of three absorbing media, water vapor, carbon dioxide and ozone, whose absorption bands are composed of many lines which are subject to pressure broadening.

Some remarks must be added here as to the vertical distribution of water vapor. Under the obtained temperature distribution shown above the water vapor will be supersaturated at some lower levels and it will accordingly condense. The modification of the vertical distribution of water vapor thus aroused will necessarily result to the modification of the equilibrium temperature distribution too. Strictly speaking, the vertical distribution of water vapor which was assumed by the writer to be as it really happens in the atmosphere is not based on any physical ground. It will be largely modified by the temperature distribution which we want to determine, and from the physical ground both the water vapor and the temperature distributions must be simultaneously determined to be compatible with each other. However, as will be seen in Table 2, the essential characteristics of the finitely thick atmosphere is that the possible temperature range which the atmosphere can take diminishes with decrease of the optical thickness of the atmosphere. And it is certain that the total water content of the atmosphere decreases with increasing latitude, and it is also highly probable that the total water vapor content will not be so much different from the actual one whatever the vertical distribution may be. In these circumstances it will be said that, even if the distribution of water vapor were otherwise assumed, the distribution of the temperature calculated would not be much differed from the above calculated one, provided that the total water vapor content in the air column be unchanged.

##### 5. Pressure Effect in the Grey Case.

The effect of the pressure broadening of infrared lines on the transfer of radiation in our atmosphere has been emphasized by STRONG and PLASS. According to them the pressure effect causes lower layers of the atmosphere to lose considerably more radiation to space than is the case when the line character is ignored. The mechanism is that the lower layers are cooled by radiation to cosmic cold more strongly than are the upper layers because the pressure effect exposes the wings of the absorption lines in the lower layers almost unobstructedly to the cosmic cold, while the radiations which are emitted near the line centers are strongly absorbed by higher layers. Thus the pressure effect is deeply connected with the line character of absorption bands. And from the above argument it may be clear that the very combined effect of the line character of infrared absorption bands and the pressure broadening of lines plays an important rôle on the transfer of radiation in our atmosphere. Accordingly the assumption of the pressure effect in the grey case is to some extent unnatural, and it may be approved only as the extreme case in which the distribution of lines is

sufficiently thick to form a nearly continuous spectrum. In such a case the pressure correction is approximately to replace the water content  $u = \int_0^p \frac{q}{g} db$  by the effective water content  $u^* = \int_0^p \frac{q}{g} \frac{p}{p_0} dp$  ( $p_0 =$  the standard pressure) on the assumption that the pressure effect is proportional to pressure. The temperature distribution was calculated with use of the effective water content for LONDON'S model atmosphere and it was shown in Table 5. If we define the tropopause by the same procedure as

Table 5. The calculated temperature distribution with pressure correction. The effective

vapor content is given by  $u^* = \int_0^p \frac{q}{g} \frac{p}{p_0} dp$ , and the optical thickness is given by  $\tau = ku^*$  with  $k = 0.5$ .

0 - 10°N. $T_s = 300.9$			20 - 30°N. $T_s = 295.5$		
Level (km)	$u^*$	$T$	Level (km)	$u^*$	$T$
0	3.8697	289.3	0	2.3258	277.9
1	2.1867	258.0	1	1.2258	250.2
2	1.2547	238.5	2	0.5758	227.3
3	0.7107	224.4	3	0.2964	220.1
4	0.3907	213.0	4	0.1448	212.6
5	0.2020	204.9	5	0.0701	208.4
7	0.0381	196.2	7	0.0150	204.6
9	0.0096	194.4	9	0.0027	203.6
11	0.0016	193.9	11	0.0006	203.4
13	0.0003	193.9	13	0.0002	203.3
15	0.0001	193.8	15	0.0001	203.3
$\infty$	0	193.8	$\infty$	0	203.3

40 - 50°N. $T_s = 277.2$		
Level (km)	$u^*$	$T$
0	0.9496	252.3
1	0.5586	236.8
2	0.2971	225.0
3	0.1421	216.8
4	0.0657	212.3
5	0.0299	209.9
7	0.0063	208.2
9	0.0021	207.9
11	0.0010	207.8
$\infty$	0	207.7

60 - 70°N. $T_s = 258.9$		
Level (km)	$u^*$	$T$
0	0.2505	225.7
1	0.1555	219.9
2	0.0564	212.9
3	0.0474	212.1
4	0.0226	210.1
5	0.0130	209.2
7	0.0049	208.5
9	0.0021	208.2
$\infty$	0	208.0

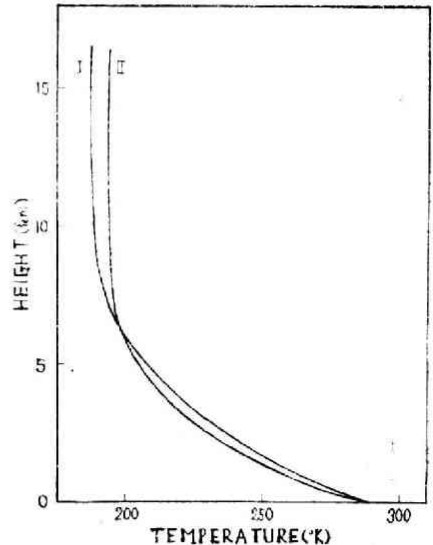


Fig. 5. Illustration of the pressure effect in the grey case.

I: The temperature profile at 0-10°N in the case of the pressure-independent absorption.

II: The same in the case of the pressure dependent absorption.

Table 6. The height and the temperature of the tropopause for the LONDON'S model atmosphere with pressure correction.

Latitude	Height (km)		Temperature (K)	
	Observed	Calculated	Observed	Calculated
0 - 10°N	16.0	16.3	197.5	193.8
20 - 30°N	16.0	14.2	201.4	203.3
40 - 50°N	11.0	10.7	218.0	207.8
60 - 70°N	10.0	7.8	220.7	208.5

was described in the preceding section the height and the temperature of the tropopause will be as shown in Table 6. In this case the discrepancy between the observed and the calculated temperature at each latitude is smaller than that in the previous case.

Finally the effect of pressure correction in the grey case is most clearly illustrated in Fig. 5, in which the temperature profiles at 0~10°N both in the case of the pressure-independent absorption and in the case of the pressure-dependent absorption are drawn. Thus the stabilizing effect of the pressure correction is evident even in the grey case.

*Acknowledgement.* — The writer wishes to note his gratitude for the financial support given by the Ministry of Education. He also thanks heartily to Miss S. SUZUKI for her helps on numerical computation.

#### References

1. CHANDRASEKHAR, S. : *Radiative Transfer*. Oxford, (1950)
2. DOBSON, G.M.B., BREWER, A.W. and CWILONG B. M. : Meteorology of the lower stratosphere. *Proc. Roy. Soc.* 185, 144, (1946)
3. EMDEN, R. : Über Strahlungsgleichgewicht und atmosphärische Strahlung. Ein Beitrag zur Theorie der oberen Inversion. *Sitz. d. K. Bayerischen Akad. d. Wiss. z. München*. S. 55, (1913).
4. GOODY, R. M. : The thermal equilibrium at the tropopause and the temperature of the lower stratosphere. *Proc. Roy. Soc.* 197, 187, (1949).
5. KOURGANOFF, V., and BUSBRIDGE I.W. : *Basic Methods in Transfer Problems*. Oxford, (1952).
6. LONDON, J. : Study of the atmospheric heat balance. *A.F. progress Reports*. 131.01—05. New York Univ. (1950—1951).
7. Strong, J., and PLASS G.N. : The effect of pressure broadening of lines on atmospheric temperature. *Astrophys. J.*, 112, 365, (1950).
8. YAMAMOTO, G. : On a Radiation Chart. *Sci. Rep. Tohoku Univ. Ser. 5. Geophys.* 4, 9, (1952).
9. ————— : Effect of radiative transfer on the vertical distribution of temperature in the troposphere. *Sci. Rep. Tohoku Univ. Ser. 5. Geophys.* 4, 64, (1952).